TECHNICAL RESEARCH REPORT

Efficient Resource Utilization through Carrier Grouping for Half-duplex communication in GSM-based MEO Mobile Satellite networks

by Iordanis Koutsopoulos, Leandros Tassiulas

CSHCN TR 2001-11
(ISR TR 2001-18)

The Center for Satellite and Hybrid Communication Networks is a NASA-sponsored Commercial Space Center also supported by the Department of Defense (DOD), industry, the State of Maryland, the University of Maryland and the Institute for Systems Research. This document is a technical report in the CSHCN series originating at the University of Maryland.

Web site http://www.isr.umd.edu/CSHCN/

Efficient Resource Utilization through Carrier Grouping for Half-duplex communication in GSM-based MEO Mobile Satellite networks

Iordanis Koutsopoulos, *Student Member* IEEE
Leandros Tassiulas, *Member IEEE*

Abstract

In the near future, existing terrestrial radio networks are envisioned to integrate with satellite systems to provide global coverage. In order to enable communication for both non-hand-held and hand-held User Terminals (UTs), the radio link design must allow the UT to operate in full- and half-duplex mode respectively, where the latter is desirable when radiation power restrictions are imposed. In addition, sophisticated resource management and diversity provisioning will enhance system capacity and reliability. However, propagation delay caused by the satellite link may lead to inefficient resource allocation and problematic diversity provisioning. In this paper, we address and study the resource allocation problem pertaining to a Medium-Earth-Orbit (MEO) satellite system with half-duplex communication capabilities. Such a system is characterized by large propagation delays, large intra-beam delay variations and inherently poor resource utilization. We propose a channel classification scheme, where the available carriers are partitioned into classes and each class is associated with a certain range of propagation delays to the satellite. The suggested infrastructure results in higher channel utilization, reduced call blocking rate and efficient diversity provisioning and can be implemented with low signaling load.

Keywords

Mobile satellite networks, resource allocation, synchronization, half-duplex communication, carrier frequency allocation, carrier classification, delay classes.

Resubmission for the JSAC Wireless Communications Series. Corresponding author : Iordanis Koutsopoulos

I. Introduction

Wireless communication networks are considered as the predominant expression of the evolution in telecommunications in recent years. The need for voice, data or multimedia services is constantly growing and wireless access solutions are very appealing, since they provide mobile users with access to information sources. Existing terrestrial cellular radio networks are restricted to providing communications services within limited regions. In order to extend the availability of services and guarantee global coverage, satellite systems have been proposed as a supplement to these networks. While in the coverage area of a terrestrial network, a user establishes connection to a terrestrial base station. Satellite network support is provided if the user is not covered by any terrestrial network or if terrestrial resources are insufficient. Despite the intense scrutiny and inherent difficulties in getting absorbed by the telecommunications market, satellite networks remain as the prevalent solution to the global coverage and "last-mile" bottleneck access problems.

In this paper, we focus on resource management in the satellite network. Low- and Medium-Earth-Orbit (LEO, MEO) non-geostationary satellite systems were proposed, so as to establish reliable connections for mobile terminals and facilitate global coverage [1]-[3]. Subject to such orbits, satellites continuously revolve on an orbit plane around the earth. Several satellites per orbit plane and orbit planes per satellite constellation constitute the satellite network. The traffic of a User Terminal (UT) on earth is supported by the beam of the satellite which is over the UT. When the satellite moves out of the UT's horizon and is no longer visible, the traffic must be handed over to another satellite to ensure uninterrupted connection. Two types of handover have been studied in literature: the satellite and the beam handover [4],[5]. The former occurs whenever visibility of the serving satellite relative to the UT is obstructed, while the latter is activated when the UT moves into the coverage area of another beam in the serving satellite.

The problem of channel allocation in a satellite network can be stated in the same context as that in terrestrial cellular networks: Given a number of mobiles with resource requirements and given the amount of available resources (channels) in the system, allocate them to users so as to satisfy their requirements and respect potential resource reuse constraints. Resource allocation algorithms can be broadly classified in two categories, Fixed Channel Allocation (FCA) and Dynamic Channel Allocation (DCA). In FCA, a fixed

number of channels is assigned a priori at each beam or satellite, whereas in DCA, channels are assumed to reside in a common pool and each channel can be used in any beam and satellite, subject to reuse constraints. Due to dynamicity of satellite movement, handover and channel allocation are interrelated. Several channel allocation methods for terrestrial systems can be used in satellite systems [6],[7]. The "guard channel" concept in [8] uses a reservation of a fixed or dynamically adjustable number of channels for handovers, while in [9], the idea of queuing of handover requests is proposed for a user that is in the overlap area of two cells.

As a step towards integration of satellite networks and existing terrestrial ones that use the Global System for Mobile communications (GSM), multiple access schemes in the former are also defined by GSM standards [10]. GSM uses a combined time/frequency division multiple access (T/FDMA) scheme. Channel allocation consists of carrier frequency and timeslot allocation to the user and it is performed at the satellite gateway (GW), based on real-time measurements. Different channels are assigned to the forward (GW to UT) and return (UT to GW) link. An efficient resource assignment algorithm leads to high resource utilization and reduced call blocking probability. In addition, diversity enhances system reliability, by maintaining a backup path for cases of unpredictable blockage [11]. Diversity allows seamless switching between two alternative paths, by always selecting the path that provides the best signal quality. Clearly, diversity can be considered as a waste of resources, since the diversity channel can be used to carry another call. However, increased connection reliability often justifies this approach.

Recently, the GSM-based Intermediate Circular Orbit (ICO) MEO mobile satellite system was proposed to provide ubiquitous coverage. In general, MEO mobile satellite systems are characterized by large propagation delays and large intra-beam delay variations, due to the high altitude of satellites and the curvature of the earth surface. In a beam of a MEO satellite, traffic bursts from calls in different locations within the beam experience different time offsets between their transmission and reception times, due to different propagation delays of the call locations. Calls that are assigned to the same carrier frequency must experience similar time offsets, so that they can be assigned to contiguous slots. If this mechanism is not applied, a significant number of slots remains unexploited and call blocking ratio is increased.

In [12], an efficient slot assignment algorithm for geostationary satellite networks is proposed, based on the definition of coverage zones and arcs in a spot beam. Inspired by this method, we address the problem of resource allocation that arises in MEO mobile satellite networks, and especially in beams with large intra-beam delay variations. We focus on the case where half-duplex communication mode is employed, i.e., when transmission and reception time intervals do not overlap. Since MEO links are characterized by high transmission power, owing to the high satellite altitude, half-duplex operation will be employed for hand-held terminals to maintain consistency with radiation standards. We propose a method for intra-beam carrier classification and allocation to users, where the key idea is that users with similar propagation delays must be assigned the same carrier. We also study the arising issues of synchronization and user position determination in this context [13]. The proposed scheme is shown to alleviate the undesirable effect of large intra-beam delay variations of MEO networks and achieve reduced call blocking ratios.

The paper is organized as follows. In sections II and III, we define the model, provide the motivation for our study and introduce the concept of delay classes. The problem of resource allocation in the context of delay classes is identified in section IV. Section V focuses on the issue of UT assignment to a delay class, based on its position. In Section VI experimental results in terms of blocking rate, position determination accuracy and handover rates are illustrated. Finally section VII concludes our study.

II. System Definition

A. Mobile satellite network setup

A satellite constellation of K satellites in MEO orbit is considered, with no inter-satellite links (ISLs). The projection of a satellite position on the earth is defined as the *sub-satellite point*. Each satellite footprint has M beams, $B_1, B_2, \ldots, B_M$, which can be classified in L groups $\mathcal{B}_1, \mathcal{B}_2, \ldots, \mathcal{B}_L$. A group $\mathcal{B}_i$ contains all equidistant beams from the sub-satellite point. Beams belonging to subset $\mathcal{B}_i$ are referred to as *type-i* beams, for $i = 1, 2, \ldots, L$. Thus, subset $\mathcal{B}_L$ contains the out-most (edge) beams and subset $\mathcal{B}_1$ includes only the nadir (central) beam. Thus, in the footprint depicted in Figure 1, the set of type-1 beams includes beam 19, type-2 set consists of beams 18, 25, 26, 20, 13 and 12 and type-3 set includes beams 17, 24, 30, 31, 32, 27, 21, 14, 8, 7, 6 and 11. The eighteen out-most beams in the footprint are the edge

beams.

We consider a projection of the earth globe onto a two-dimensional plane. The plane is divided into squares of given longitude and latitude bounds. Satellite gateways (GWs) constitute the satellite access points for users. Each satellite provides its ephemeris data to all GWs during its revolution. The ephemeris data is simply the satellite location with respect to a reference coordinate system. A GW contains the Land Satellite Resource Management System (LSRMS), in which satellite resource management is performed. The LSRMS includes the Handover Management (HOM) and Dedicated Channel Management (DChM) software modules, in which handover and channel allocation decisions are taken. We use the terms "call" and "User Terminal (UT)" interchangeably to refer to users. Consider a pair of UTs that establish connection. User 1 transmits and receives information via a satellite that covers the UT location, and the satellite is connected to a GW. The elevation angle θ of the satellite with respect to the UT is the angle between the UT horizon and the line that connects the satellite to the UT. The UT horizon is defined as the plane which is tangent on the earth surface at the UT position. Similarly, user 2 establishes a connection with another satellite, which communicates with a GW. The GWs perform all the required processing and are interconnected with a backbone wire-line network. In general, serving satellites and GWs are different for the two users. In this paper, we focus only on the link from a satellite to a UT.

B. Access, timing and synchronization systems

A combined FDMA/TDMA access scheme is considered, based on GSM standards. A frequency band is divided into m carrier frequencies, according to FDMA scheme. Within each carrier, a TDMA structure is embedded: users share the same carrier frequency by accessing the channel in orthogonal timeslots. We assume that a TDMA carrier frame has N_s timeslots, each of duration T_s and that a user's traffic burst occupies one slot. A channel is perceived as a distinct carrier-slot pair.

In order to ensure fairness and guarantee that no carrier reassignments occur during the call, we assume that a UT transmits and receives once in a frame period of the associated carrier. Moreover, we allow for diversity provisioning within the same carrier for a user. Under half-duplex diversity operation, the number of slots per TDMA frame must be a multiple of six, the rationale being that each slot must be occupied

by a user. The minimum number of slots per frame is $N_s = 6$, in which case one user occupies a carrier in half-duplex mode and is granted diversity. Indeed, since the UT transmits and receives once in a frame and there is a guard time $t_g << T_s$ between transmission and reception intervals, three slots are required for single-path half-duplex operation, and six slots are needed if we include diversity. In this study, we assume that $N_s = 6$, which means that one user is assigned to a carrier and the assignment of multiple users in the same carrier is not an issue. It also implies that, in case of diversity, both paths are provided to a user through the same carrier. The timing and synchronization on a traffic channel (TCH) are feasible through a time reference, the "system time", defined by equally spaced time instants $\{t_0, t_1, \ldots, t_n, t_{n+1}, \ldots\}$, which coincide with the beginning of a slot. The reference time interval n is the interval $[t_n, t_{n+1}]$ and the reference window n (i.e., sequence of three contiguous slots) is the interval $[t_n, t_{n+3}]$. Windows serve as references on the earth for the timing of transmitted and received bursts at the UT.

III. Motivation of study and proposed solution

A. Problem Description

Consider a user which is assigned to a carrier. Transmission (Tx) and reception (Rx) traffic bursts of that user are separated by a time offset, which we call "Tx/Rx burst offset". Non-overlapping transmission and reception intervals for half-duplex operation are required, so that power constraints for hand-held terminals are satisfied. Under the adopted timing and synchronization assumptions, transmitted and received bursts by a UT must be accommodated within a reference window, in order to ensure better resource utilization.

The relative positions of the transmitted and received bursts in a reference window at the UT depend on the Tx/Rx burst offset. The offset value is a function of burst reception time at the UT, which in turn depends on the UT propagation delay T_p to the satellite. Users located in different positions within a beam have different propagation delays to the satellite and thus require different Tx/Rx burst offsets to maintain non-overlapping transmission and reception intervals. If these users are assigned to the same carrier, different time offsets will lead to inefficient utilization of slots in the serving carrier, since several slots will remain unoccupied. In Figure 2, the situations of a single offset value or multiple offset values within a carrier are illustrated. Clearly, in the case of a single Tx/Rx burst offset, efficient call accommodation is

achieved by "packing" users in contiguous timeslots, so that the available resource (time) is fully exploited. However, in the allocation of users with large delay variations, the system unavoidably resorts to multiple burst offsets to maintain orthogonal consecutive channels and non-overlapping transmission and reception bursts. As a result, a significant amount of resources is unutilized (in the figure, slots marked with "X"). This leads to an increase in blocking rate, since fewer calls can be accommodated in the system.

In MEO mobile satellite systems, this situation arises in beams which demonstrate large intra-beam delay variations. Edge beams which become elongated because of the curvature of the earth surface are primarily affected. In a carrier of such a beam, transmission and reception bursts will be misplaced and may not be accommodated in a reference window, thus affecting other bursts. In order to circumvent this difficulty, we define a range $\delta T_p \geq 0$ of delay variation around a nominal delay T_0. Transmission and reception bursts of UTs with propagation delays in the range $[T_0 - \delta T_p, T_0 + \delta T_p]$ will be accommodated within a reference window. UTs with propagation delays within this range are said to belong in the same *delay class* and should be allocated to the same group of carriers to avoid inefficient resource utilization.

Figure 3 illustrates the relative position of the transmission and reception bursts for three users of the same delay class, with propagation delays $T_0 - \delta T_p$, T_0 and $T_0 + \delta T_p$ respectively. A diversity path through a second beam and satellite is assumed. The nominal delay T_0 corresponds to a symmetric placement of transmission and reception bursts in the window (Figure 3b). Depending on the value of propagation delay, the transmission and reception intervals appear as "sliding" in the reference window. A small guard time t_g between transmission and reception bursts accounts for UT transmit/receive switching, frequency oscillator re-tuning and residual timing errors and is of the order of microseconds. The range δT_p of the delay class can be derived by considering the upper and lower bound of delays, within which accommodation in a reference window is feasible. We find that

$$\delta T_p = \frac{T_s}{4} - \frac{t_g}{2}. \tag{1}$$

To see this, consider a reference window with time margin t_g between Tx/Rx bursts. In order to ensure non-overlapping transmission and reception bursts for the two diversity paths of a UT, a time margin of $t_g/2$ from the starting and ending points of the window must be applied. Let $R = 2\delta T_p$. Then, from Figure

3 we have that, $2T_s + 2t_g + 2R = 3T_s$, and (1) follows readily. Transmission and reception intervals begin at time instants

$$sub-satelliteT_{TX} = 6.25T_s + T_p - T_0 \,(\mathrm{mod} N_s) \quad \text{and} \quad T_{RX} = 1.75T_s + T_p - T_0 \,(\mathrm{mod} N_s), \tag{2}$$

where by convention, reception intervals precede transmission ones. These results can be generalized for any TDMA scheme with $N_s \neq 6$ slots per frame.

B. Proposed solution

In order to provide the aforementioned solution to UTs in different locations in the satellite footprint, several delay classes and thus nominal values $T_{0,i}$ must be defined. Each delay class will constitute a class of carriers $\mathcal{C}_i$ and the propagation delay T_p of mobiles assigned to carriers of class $\mathcal{C}_i$ must satisfy,

$$T_{0,i} - \delta T_p \leq T_p \leq T_{0,i} + \delta T_p, \tag{3}$$

where δT_p is the delay class range, defined in (1). Pictorially, each nominal delay value $T_{0,i}$ corresponds to a contour (circle) on the earth surface. All nominal delay values represent concentric circles, centered at the sub-satellite point Q (Figure 4). A contour of delay $T_{0,i}$ consists of all points on earth with the same delay to the satellite. The two contours of delay $T_{0,i} \pm \delta T_p$ form a "zone", which is defined to be the *delay class i*. Bursts of UTs belonging in a delay class are arrive aligned at the satellite interface. Offset values for a specific UT are derived by comparing the UT's propagation delay T_p and the nominal delay value $T_{0,i}$ of its delay class. The offset value should be proportional to $T_p - T_{0,i}$.

Consider now the beam pattern of a satellite. Delay classes have certain positions with respect to this pattern in the footprint. Figure 5 illustrates a projection of one quadrant of the beam pattern on a two-dimensional plane and the relative position of the delay classes. We observe that beams that are closer to the footprint edge become elliptical and more elongated, and therefore comprise a wider range of propagation delays. Each delay class serves a certain set of beams, and, in particular, beams of the same beam type $\mathcal{B}_j$, due to circular symmetry. Beams of a beam type may be covered by more than one delay class. For example, out-most beams are covered by three delay classes, since propagation delay range is large. Intermediate beams may be served by one or two delay classes. Note also that beams of different

beam types that are located close to the point may be served by only one delay class. For beams with more than one delay class, an intra-beam handover event is equivalent to call transition from one delay class to another within the same beam.

Satellite resources consist of carriers, which are assumed to belong to a pool and are assigned on a per beam basis with DCA or FCA schemes. Dynamic schemes are more appropriate for non-geostationary satellite movement and traffic variations. The assignment of carriers to delay classes and the resulting Tx/Rx burst offsets that follows user allocation to these carriers results in more efficient carrier utilization. Within a satellite footprint, and under spatially uniform call distribution, the expected amount of traffic in out-most beams is larger, since these beams are elongated. This phenomenon leads to inefficient resource management, due to increased call blocking in these beams. The delay class concept can be used to alleviate this problem, by spatially distributing carriers to serve users in these beams. Thus, more delay classes and therefore more carriers are dedicated to out-most beams to carry the increased amount of traffic.

System design parameters such as the total number of delay classes κ and the exact delay class positions are computed by considering several other parameters, such as satellite orbit and height, footprint and beam size, frame structure, traffic burst length, and even guard time t_g. Since adjacent delay classes may overlap, the maximum residence time at a delay class overlap area is another important design parameter that affects delay class positions. This residence time represents the maximum allowed tolerance for delay class handovers. Owing to large complexity, we will not attempt to derive a standard methodology for the determination of delay class positions in the footprint. Instead, we focus on the issue of determining the serving delay class for a call, which is crucial for resource allocation. In Appendix A we provide a simple heuristic (Algorithm C) for the determination of time delays $T_{0,i}$, corresponding to delay classes. We also assume that carriers are allocated a priori to delay classes.

IV. Delay Class determination and resource allocation

A. Problem Statement

When a call is initiated, resources are assigned to it after a call request message, which contains the current satellite and beam identities and the propagation delay to the satellite. On the other hand, resource

allocation for an ongoing call is associated with handover events, since the call is then transferred to another channel. In order for a new channel to be assigned to a call, the HOM software unit of the LSRMS requests the resources from the DChM software unit, while providing the current satellite, beam and delay class identities. DChM then allocates resources to the call on a per beam and delay class bases.

If a beam or a delay class handover occurs, determination of the new delay class is feasible because timing to the current satellite is maintained. However, in the event of a satellite handover, synchronization is lost, since satellite synchronization systems are independent from one another. Although a satellite handover event is less frequent than a beam handover one [5], it can certainly occur, since satellite footprints move fast on the earth surface. A satellite handover also occurs in the case of a call with long duration, or a call located at an edge beam. The derivation of the new delay class (i.e., propagation delay) in the new satellite is vital in keeping track of the UT through system timing and proceeding to reliable resource assignment. Two methods can be used by the LSRMS to determine the new value of propagation delay:

- METHOD 1: The LSRMS retrieves from its memory the most recent estimate of UT position and associates it with the new satellite ephemeris data, to derive a new estimate of the delay.
- METHOD 2: The LSRMS requests a measurement report from the UT. In that mode, the LSRMS provides the UT with the rough propagation delay information with respect to the new satellite. The UT then measures the message delay relative to the new satellite and reports the difference between the actual and rough propagation delay, $T_p - \tilde{T}_p$, with respect to the new satellite back to the LSRMS, which can now determine the new propagation delay with high accuracy.

The first method is faster and easier to implement. The second method is more accurate but is also time- and bandwidth-consuming, because of the large amount of exchanged information. Therefore, the first method should be given priority and used whenever the estimated UT position is accurate enough to provide a reasonable estimate of the delay. A UT position error is acceptable if it does not invoke a misleading result for the identity of the current delay class, as will be discussed in the next subsection. If the UT position estimate is not accurate enough, then the system should resort to the second method. We consider the case of satellite handover, in which determination of delay from the UT to the new satellite is

crucial in resource allocation, and use one of the two methods above to determine the delay. The question that arises is when to use each method, so as to minimize the incurred signaling load.

B. UT position error tolerance region

Each UT is characterized by a unique *actual* location on the earth and a unique time delay to a satellite. However, we assume that only estimates of the above quantities are available. Estimated UT position is also called *known UT position*. Consider a beam which is located far enough from the sub-satellite point, so that it is covered by two delay classes (Figure 6). Let the delay classes correspond to two zones defined by delays $T_{0,i} \pm \delta T_p$, for $i = 1, 2$. Assume that $T_{0,1} < T_{0,2}$, so that the first (inner) delay class is closer to the sub-satellite point Q. When the UT is located in regions 1 or 2, it is assigned to a carrier of the corresponding delay class (1 or 2). Region 3 corresponds to the time delay interval $I_{ov} = [T_{0,2} - \delta T_p, T_{0,1} + \delta T_p]$, and it is the overlap region of the two delay classes. Delay variation δT_p determines the length of the delay class overlap region and is independent of the delay class, unless we define different lengths of delay class overlap regions. We can also change the overlap region of delay classes simply by changing their position.

While in the overlap region, the UT can be served by carriers of delay class 1 or 2. By applying diversity, the best carrier out of the two eligible groups of carriers is selected to serve the UT. Based on its instant time delay, the UT may belong in one of the three depicted regions in a beam. However, because of inaccuracy in delay evaluation, the UT may *seem* to reside in a different region from its actual one. Specifically,

- If the UT's actual position is in region 1, then the wrong delay class 2 is assigned, either if the known UT position is in region 2, or if the known UT position is in region 3 and delay class 2 is selected.
- If the UT's actual position is in region 2, then the wrong delay class 1 is assigned, either if the known UT position is in region 1, or if the known UT position is in region 3 and delay class 1 is selected.
- If the UT's actual position is in region 3, then either of the two delay classes may serve the call. In the worst case, there will be a delay class handover without undesirable consequences.

Therefore, an incorrect delay class assignment occurs only when the difference between the actual and the known position corresponds to a propagation delay difference, that is greater than the length of the overlap region. In order to investigate an incorrect delay class assignment, one has to determine the length

of the delay class overlap regions in the new beam, after the satellite handover. For a beam with n delay classes, there are $n-1$ overlap regions. Finding the minimum length overlap region and converting it to distance corresponds to computing the worst case error in position determination that will not lead to incorrect delay class assignment. The correct delay class must be allocated to the call, so that the UT is assigned to an appropriate carrier. We propose the following methodology to solve the problem:

ALGORITHM A: COMPUTATION OF UT POSITION TOLERANCE REGION

- STEP A : Divide the set of satellite beams into subsets $\mathcal{B}_1, \mathcal{B}_2, \ldots, \mathcal{B}_n$, so that each beam in $\mathcal{B}_j$ has κ_j delay classes. Beams of subset $\mathcal{B}_i$ are type-i beams and form a toroid.
- STEP B : For each pair of adjacent delay classes i and $i+1$ that serves beams of $\mathcal{B}_j$, find the time lengths x_{ij} of the overlap regions, given by $x_{ij} = T_{0,i} - T_{0,(i+1)} - 2|\delta T_p|$, where $T_{0,i} > T_{0,(i+1)}$. For subset $\mathcal{B}_j$ with κ_j delay classes, $i = 1, \ldots, \kappa_j - 1$. Then, for each subset $\mathcal{B}_j$ select $x_j = \min_{i=1,\ldots,\kappa_j} x_{ij}$, to account for the worst case scenario (minimum length overlap region) for a beam with several delay classes. Clearly, x_j is the maximum allowed inaccuracy between the actual and the estimated time delay, for beams of subset $\mathcal{B}_j$, so that incorrect delay class assignment is avoided. In other words we have,

$$x_j = \hat{e}_{max,j} = \max_k |T_{p_k} - \tilde{T_{p_k}}|, \tag{4}$$

where T_{p_k} and $\tilde{T_{p_k}}$ are the actual and estimated delays for user k in subset $\mathcal{B}_j$.

- STEP C : Compute the tolerance in the UT-satellite path distance, given as $\Delta d_j = c \cdot \hat{e}_{max,j}$, where $c = 3 \times 10^8$ m/sec is the light velocity.
- STEP D : For each subset $\mathcal{B}_j$ and each delay class $i = 1, \ldots \kappa_j$, compute the two "extremes" of path lengths to the satellite, $d^{\pm}_{i,j} = c \cdot T_{0,i} \pm \Delta d_j$, as shown in Figure 7. Then, compute the associated central angles by using the law of cosine, [14]:

$$\theta^{\pm}_{i,j} = \frac{R_E^2 + (R_E + H)^2 - \left(d^{\pm}_{i,j}\right)^2}{2R_E\,(R_E + H)} \tag{5}$$

where R_E is the earth radius.

• STEP E : Compute the radius of each circular tolerance region, $L_{i,j} = (R_E/2)\left|\theta_{i,j}^{+} - \theta_{i,j}^{-}\right|$, and for that set of beams with κ_j delay classes, select $L_j = \min_{i=1\ldots\kappa_j} L_{i,j}$, to account for worst-case error.

In Step E, the assumption of a "locally flat horizon" on the earth surface was used. This assumption is valid, since an arc on the earth can be considered flat for arc lengths $\ell << R_E$. Then, we applied the formula that gives the length ℓ of an arc of central angle ω on a circle of radius R, as $\ell = R\omega$.

C. Assignment of the correct delay class

We now describe the sequence of procedures in order to select the appropriate method (method 1 or method 2 of section IV.A) and proceed to assignment of the correct delay class. Delay class assignment to a UT is equivalent to estimation of UT position. The region in which the UT resides (delay class overlap or non-overlap region) and UT position uncertainty $|T_p - \tilde{T}_p|$ will determine the method to be used.

The estimate of the UT position is generated by means of simulation for simplicity. We assume that the actual delay and Doppler frequency offset values are available and the estimated UT position is derived from estimates of delay and Doppler frequency, which are randomly distributed around the actual values, according to a Gaussian distribution. UT position determination by means of delay and Doppler frequency values is outlined in Appendix B. Let UT_{act} and UT_{known} be the actual and known positions of the UT, and assume that the beam has $n > 1$ delay classes, so that correct delay class assignment is an issue. The known UT position will correspond either to a non-overlap delay class region k, $k = 1, \ldots, n$, or to an overlap region ℓ, between delay classes ℓ and $\ell + 1$, $\ell = 1, \ldots, n-1$. In the first case, method 1 can be used if UT position inaccuracy is less than the minimum length overlap region for that particular beam type. In the second case, we need to compute the parameters

$$\tau_1 = T_{0,(\ell+1)} + \delta T_p - \tilde{T}_p \quad \text{and} \quad \tau_2 = \tilde{T}_p - (T_{0,\ell} - \delta T_p) \tag{6}$$

which denote the distances of the known position from the two sides (delay bounds) of the overlap region. The procedure to make a delay class assignment is as follows:

ALGORITHM B: DERIVATION OF METHOD FOR DELAY CLASS ASSIGNMENT

• STEP 1 : Execute Algorithm A of section IV.B to derive tolerances L_j for each beam subset $\mathcal{B}_j$.

- Step 2 : For every UT in the satellite footprint, execute steps 3-6 below.
- Step 3 : Compute the actual propagation delay and Doppler frequency offset.
- Step 4 : Generate delay and Doppler frequency offset values, based on Gaussian distribution and derive the estimated (known) UT position.
- Step 5 : Compute the distance between the estimated and the actual UT position and determine the beam and beam type $\mathcal{B}_m$ of the known UT position.
- Step 6 : Distinguish between the following cases:
  - Case 6A: Known delay $\tilde{T}_p$ corresponds to a known UT position in a non-overlap region ℓ.
    - Case 6A.1: If $|UT_{act} - UT_{known}| < L_m$, then use method 1 to find the delay.
    - Case 6A.2: If $|UT_{act} - UT_{known}| \geq L_m$, then use method 2 to find the delay.
  - Case 6B: Known delay $\tilde{T}_p$ corresponds to known position in an overlap region ℓ.
    - Case 6B.1: If $|UT_{act} - UT_{known}| < \min\{\tau_1, \tau_2\}$, then use method 1 to find the delay.
    - Case 6B.2: If $|UT_{act} - UT_{known}| \geq \min\{\tau_1, \tau_2\}$, then use method 2 to find the delay.

Step 6 : Use that delay value to assign the call to a delay class.

In the case where parameters τ_1 and τ_2 are computed, $\min\{\tau_1, \tau_2\}$ is the closest distance from the overlap region boundary. The condition $|UT_{act} - UT_{known}| \geq \min\{\tau_1, \tau_2\}$ means that the error region covers the overlap region ℓ and part of non-overlap regions ℓ or $\ell + 1$. In such a case, only method 2 can guarantee a correct delay class assignment. Otherwise, if $|UT_{act} - UT_{known}| < \min\{\tau_1, \tau_2\}$, the error region lies entirely in overlap region ℓ and method 1 can be used.

V. Simulations and results

A. Simulation parameters

To back up the analysis of previous sections, a discrete event simulator of a MEO mobile satellite system was built. We followed the specifications of the ICO satellite system. The constellation consists of 10 satellites at an altitude of $10,300$ km above the earth surface. There exist two orbit planes and five satellites per orbit plane. Each orbit plane is inclined 45 degrees with respect to the equatorial plane. A satellite footprint has 163 beams, which can be partitioned in eight beam types. A UT can be served by a

satellite when the satellite elevation angle θ with respect to the UT exceeds a threshold angle θ_{min}, which specifies the visibility conditions. We assume that $\theta_{min} = 10^o$, which can be considered as a realistic value for a rural environment. For an urban environment, this threshold would be higher. The elevation angle for a UT in an edge beam is low and increases as the UT moves towards the central (nadir) beam. The maximum elevation angle of 90 degrees is then achieved. Within each satellite footprint, the positions of the delay classes were computed by Algorithm C, which is presented in Appendix A. Thus, concentric rings as these in Figure 4 are defined, each of which corresponds to a certain elevation angle to the satellite. In order to serve beams close to the sub-satellite point with one delay class, we set the closest delay class to be the ring corresponding to elevation angle of 60 degrees. By applying the delay class position determination algorithm, we found that the maximum number of delay classes that ensures coverage of a beam is 3. Thus, beams can be covered by one, two or three delay classes. By executing algorithm A, the distance tolerance values that guarantee correct delay class assignment for beams with two and three delay classes were found to be $142km$ and $24km$ respectively. Thus, position determination is more sensitive in beams with three delay classes, due to closeness of delay classes and reduced length of overlap regions.

UTs reside in the coverage area of one GW for simulation, so that GW handover events are not considered. In the simulated environment, satellite, beam and delay class handovers can occur. In satellite handover, two strategies have been proposed in literature [15]: According to the first one, a UT always selects the satellite that provides the highest elevation angle. This strategy maximizes the instantaneous elevation angle to reduce blockage probability. Another approach instructs that a UT must constantly select the same satellite, as long as it remains visible. This method minimizes satellite handover rate, and thus reduces signaling load. In this study we adopt the second strategy, firstly because elevation angle may be low at a rural environment, and secondly because a low satellite handover rate diminishes the probability of incorrect resource assignment (recall that the correct delay class assignment problem appears upon satellite handover). A beam handover occurs when a UT moves in the coverage area of a beam other than the current one, within a satellite. Since beams overlap in the beam pattern (Figure 1), a beam handover occurs in a random time instant, during the time that the UT is in the beam overlap area. Similarly, a

delay class handover occurs when the UT moves to another delay class within a beam. Again, the handover occurs during the time the UT is in a delay class overlap area.

We simulated an one-hour continuous revolution of satellites on their specified orbit. A base frequency of f of 2.01 GHz was considered and several carrier frequencies were defined. Calls in different beams are assumed to arrive in independent Poisson streams of equal rate λ and have exponentially distributed durations, with mean $\tau = 1/\mu = 150sec$, which is typical for voice transactions. Traffic intensity for each beam is measured in Erlangs (E), as $E = \lambda\tau/60$. Although handover events are affected more by velocities of moving satellites rather than UT movement, a simplistic UT mobility model is used. A random number of UTs is assigned a velocity, whose magnitude is uniformly distributed between 0 and 72 km/h and the direction of motion is uniformly distributed between 0 and 2π. Velocity magnitude and direction are updated several times during a call. The remaining percentage of UTs are assumed to be fixed. Diversity attributes are provided to a maximum percentage 40% of calls, whenever more than one paths are available. Frame duration is assumed to be $T_f = 40msec$ and each frame consists of six timeslots, each of duration $T_s = 6.67msec$. All connections are half-duplex and all transactions are voice calls.

B. Improvement in call blocking rate

In previous sections it was mentioned that the proposed scheme of carrier grouping and application of single Tx/Rx burst offset to all carriers within a delay class of a beam leads to more efficient resource utilization and reduction of call blocking rate. The presented method does not significantly affect blocking rate in moderate size beams that are not elongated, since in these beams only one delay class is defined and carriers are not divided into delay classes. On the contrary, edge beams are characterized by large delay variations, and carrier grouping according to delay classes offers a clear advantage.

We performed experiments for such an edge beam and measured performance for randomly generated UTs within the beam area. For simplicity, we considered a fixed channel allocation scheme, namely the number and identities of carriers allocated to that beam were fixed. The propagation delays from UT positions to the satellite were computed. In a first simulation scenario, we ran the simulation without adoption of the proposed carrier grouping scheme. UTs were allocated randomly in one carrier, irrespective

of their location in the beam. As a result, UTs assigned on the same carrier demonstrated different Tx/Rx burst time offsets, so as to maintain their orthogonality with respect to each other.

In the second scenario, the beam area was divided into three delay classes and the set of carriers was divided into three subsets. Each subset of carriers was mapped to a delay class. After obtaining the nominal delay values for delay classes, the following channel assignment method was employed: calls belonging to a certain delay class were assigned to a carrier of that delay class sequentially. That is, each time a carrier of one delay class became full, the UTs of that delay class were assigned to another carrier of that delay class. A certain Tx/Rx burst time offset was applied to calls which were served by carriers of a delay class, which was proportional to the difference of UT propagation delay and the nominal value of the delay class in which it belonged. Calls which belonged to the overlap area of two delay classes were assigned to the least loaded carrier in the set of carriers of corresponding delay classes. When all carriers of a delay class were full, the call was blocked. The blocking probability was defined as the ratio of blocked call requests over the total number of calls. Two different instances of the experiment were created, where beam resources consisted of 12 and 45 carriers respectively. Results are illustrated in Figure 8. The improvement in performance because of carrier grouping is evident. For example, in the case of 12 carriers and a traffic of 25 Erlangs, blocking probability was reduced by almost 50%. The benefit of carrier grouping is greater for high traffic loads. Calls which do not receive service in the first scenario due to waste of resources, are efficiently allocated. For a larger resource pool of 45 carriers, the advantage of carrier grouping becomes more substantial. For example, for a beam with 45 carriers and 160 Erlangs, the blocking rate was reduced by a factor of 30%, when the allocation of UTs to specific carriers was applied.

C. Estimation of UT position

The underlying problem of correct delay class assignment is UT position estimation. The accuracy of the estimation determines the allocation method and the signaling load. According to method 1, the most recently received delay is retrieved, while method 2 requests an explicit, updated estimate of delay. Several methods for estimating UT position are available by using ephemeris data from one or two satellites. Typically, UT-satellite delay and Doppler frequency shift due to satellite movement are used to determine

UT position. The following techniques can be used to determine the UT position:

- METHOD I : Using delay and Doppler frequency measurements from one satellite.
- METHOD II : Using delay and Doppler frequency measurements with the ellipsoidal earth assumption.
- METHOD III : Using one delay and the differential delay measurement of two satellites.
- METHOD IV : Using one Doppler frequency and the differential delay measurement of two satellites.
- METHOD V : Using one delay and the differential Doppler frequency measurement of two satellites.
- METHOD VI : Using one frequency and the differential Doppler frequency measurement of two satellites.
- METHOD VII : Using differential delay and differential Doppler frequency measurements of two satellites.

Method I is the method which is used traditionally for UT position determination. Method II additionally takes into account the eccentricity of earth surface, which causes changes in the projection of satellite orbit on the earth. Methods III-VII which involve two satellites are clearly more accurate but require additional computational burden. They should come into stage only if one-satellite measurements do not provide the specified accuracy and when data from two satellites are readily available. In Appendix B, the expressions of UT position by using delay and Doppler frequency measurements from one satellite are obtained, as an illustrative example of such kinds of computations. It should be noted that our study does not explicitly require use of GPS equipment, but it is not affected by GPS existence, as well. Consider the resource allocation problem of section IV. Recall that in the case of a beam or a delay class handover, the UT position and delay can be estimated with accuracy (potentially through GPS equipment). In the case of a satellite handover, GPS cannot provide a reliable estimate of UT position, if the synchronization systems of the satellites are independent. In that case, method 1 or method 2 of section IV.A must be employed.

In Table I, we present some comparative results for the accuracy of UT position estimation, with respect to the measurement method. Results were obtained by applying standard mathematical expressions for UT position determination and assuming a certain delay and frequency measurement error, as outlined in section IV.C. This essentially corresponds to an application of method 1 for UT position determination. These results can be utilized in approximating the percentage of times when methods 1 or 2 are used for correct delay class determination. If the experiment is executed for a large number of UT positions, the resulting percentages can serve as estimates of the probability that method 1 will produce reliable results.

If UT position error is less than L_j for $y_j\%$ of the time for some subset $\mathcal{B}_j$ of beams, method 1 can be safely used to determine the delay class for $y_j\%$ of time and method 2 will be used for the rest $(100-y_j)\%$ of time. We note here that UT position will always be determined with accuracy. However, application of complex method 2 will be restricted. The following conclusions can be drawn from Table I:

- The simple method 1 has excellent performance when the new beam has two delay classes, irrespective of the utilized method of measurements. Measurements from one satellite are therefore sufficient to ensure reliability. In that case Method 1 can be used almost entirely $(97\% - 98\%)$ to safely estimate delay.
- If the new beam has three delay classes and measurements from one satellite are used, method 1 gives satisfactory results for $80\% - 83\%$ of the times, irrespective of the measurement method. Method 2 can be utilized for $17\% - 20\%$ of the times, depending on the measurement method and the number of satellites.
- For the case of a beam with three delay classes, high performance can be achieved by method 1, if differential delay measurements between two satellites are used together with differential Doppler frequency or delay from one satellite. In that case, Method 1 can be used almost exclusively.
- If the known position of UT lies in the overlap region, method 2 can be used when the radius of the error region exceeds certain threshold values, which depend on the known position (see Case 6B.2 of Algorithm B). The percentage of time when method 2 is used depends on the instantaneous UT known position and delay can be easily calculated in a similar fashion.

It was also observed that measurements that involve Doppler frequency calculations demonstrated a small difference in the values above, due to UT motion. Methods which purely employ delay (absolute or differential) are more robust to mobility. Moreover, position accuracy was marginally improved when measurements were provided from two satellites with a large separation angle. For example, for method I the percentage of 83% was raised to 85% for satellites with separation angle greater that 70^o, since blockage of both paths due to obstruction is less probable when the satellite separation angle is large.

D. Handover rates

We measured the resulting handover rates in our simulation. Three kinds of handovers are involved: satellite, beam and delay class handover. Handover occurances in either of the two diversity paths were

counted as single transitions. In Figures 9 and 10 the handover rates and number of handover occurances are depicted as a function of time. Figure 9 is from a square location of $15^o \times 15^o$, within 15^o longitude and latitude distance from the GW, while figure 10 is from a $15^o \times 15^o$ square within 45^o longitude and latitude distance from the GW. Call arrival rates were $\lambda = 4.87$ calls/sec and 1.69 calls/sec respectively.

A first observation is that all handover rates converge to a steady state after a transition interval of about $2,000 - 2,500$ seconds. The number of handovers then increases linearly with time. The number of transitions depends on the induced traffic at a particular location. In steady state, we observed that about 3 and 30 delay class transitions per minute occur, when the traffic is 1.69 and 4.87 calls/sec respectively, which means that the number of beam (and therefore, delay class) transitions increases rapidly under high traffic load. The number of delay class handovers is larger in the first location, which is closer to the serving GW, since more calls are supported from the GW. In general, delay class handover rate depends on whether the UT is located in edge beams with more than one delay classes. The relative magnitude of handover rates in the steady state can be approximated as well: for locations close to the GW, the ratio of satellite, beam and delay class handover rates is $2 : 7 : 3$, while for further locations it changes to approximately $1 : 15 : 1$. The aggregate satellite, beam and delay class handover rates for all traffic carried by this GW are illustrated in Figure 11. As anticipated, handover rates behave as a smooth function of time and ultimately reach a steady-state. Delay class handover rate becomes in a way predictable, since it occurs only within prespecified beams with more than one delay class. Such graphs are very important in resource planning and forecasting in different times of the day.

VI. Conclusion

This paper presents a first attempt to identify and study an important problem which arises in MEO mobile satellite networks. We present a novel resource allocation scheme, which is applicable in such systems, which are characterized by large satellite footprints and large intra-beam delay variations. The scheme alleviates large delay variations by classifying carriers in classes and associating each group of carriers with a certain Tx/Rx burst time offset value, that depends on propagation delay. Each UT is assigned to a particular group of carriers, based on its location in the satellite footprint. The scheme

achieves reduction in call blocking rate and facilitates diversity provisioning for half-duplex connections. Subsequently, UT assignment to the appropriate delay class is identified as the fundamental problem of resource assignment under the proposed delay class scheme. We focus on delay determination in the case of a satellite handover and present two methods for UT position determination. We show that reliable resource allocation can be achieved, while the amount of signaling load is kept to a minimum, by utilizing the complicated method only when necessary.

Several directions for future study are available. A more elaborate design of delay class positions, by considering overlap regions would be worth studying. The impact of simultaneous employment of full- and half-duplex modes in the analyzed infrastructure and algorithms is also an interesting topic. Finally, the issue of more sophisticated carrier allocation methods within the satellite footprint (for example, dynamic carrier allocation under resource reuse constraints) as well as that of efficient intra-beam call assignment methods in the context of the delay class infrastructure, deserves further attention and investigation.

VII. Appendix A : Derivation of Delay Class positions

Assume that a number of delay classes κ is defined within a satellite footprint. Let θ be the elevation angle from the UT to the satellite and ϕ be the earth central angle, as depicted in Figure 12. Let d and τ be the distance and delay from a delay class contour to the satellite. Assume that H is the satellite height and R_E is the earth radius. A "cup" on the earth is the area defined by a delay class contour and a pole, and a "zone" is defined by delay class contours, i and $i+1$. Let A be the area of a cup or zone on the earth. The minimum and maximum satellite elevation angles, θ_{min} and θ_{max} stem from satellite visibility conditions and definition of the closest delay class to satellite nadir. Range $[\theta_{min}, \theta_{max}]$ represents the part of the satellite footprint to be covered with delay classes. Equivalently, this coverage area can be defined by earth central angle range $[\phi_{max}, \phi_{min}]$, where the relation between angles ϕ and θ is given by [14]

$$\phi(\theta) = \frac{\pi}{2} - \sin^{-1}\left(\frac{R_E}{R_E + H}\cos\theta\right) - \theta \ , \tag{7}$$

and $\phi_{min} = \phi(\theta_{max})$, $\phi_{max} = \phi(\theta_{min})$. The following algorithm determines delay class positions. Note that delay class overlap regions were not taken into consideration.

Algorithm C : Determination of Delay Class positions

- Step 1 : Obtain the pair $(\phi_{min}, \theta_{max})$.
- Step 2 : At first iteration, determine the first delay class:
  - Step 2.A : Compute parameter h_0 (see Figure 12) as $h_0 = R_E\,(1 - \cos\theta_{max})$. This is the height of the first (closest to satellite nadir) delay class. A cup is thus defined on the earth surface, at height h_0.
  - Step 2.B : Find the area of this cup, $A = 2\pi R_E h_0$.
  - Step 2.C : Compute the distance parameters,

$$a_0^2 = R_E^2 - (R_E - h_0)^2 \quad , \quad d_0^2 = a_0^2 + (H + h_0)^2 = H^2 + 2\,(R_E + H)\,h_0 \tag{8}$$

where d_0 is the distance from the first $(j = 0)$ delay class contour to the satellite and a_0 is as in Figure 12.

  - Step 2.D : Find the corresponding delay to the satellite, $\tau_0 = d_0/c$.
- Step 3 : At j-th iteration, determine the $(j+1)$-th delay class, $j = 1, 2 \ldots, \kappa - 1$:
  - Step 3.A : Select constant height $h_j = A/(2\pi\kappa R_E)$.
  - Step 3.B : Compute the distances

$$a_j^2 = R_E^2 - \left(R_E - \sum_{i=0}^{j} h_i\right)^2 \quad , \quad d_j^2 = a_j^2 + \left(H + \sum_{i=0}^{j} h_i\right)^2 = H^2 + 2\,(R_E + H)\sum_{i=0}^{j} h_i \tag{9}$$

  - Step 3.C : Find the delay of the $(j+1)$-th delay class to the satellite, $\tau_j = d_j/c$.
- Step 4 : Repeat this procedure for $j = 1, 2 \ldots, \kappa - 1$.

Heights h_j, which define the $(j+1)$-th delay class are selected, so that the surface area of each zone, defined by heights h_{j-1} and h_j, is equal to that of the defined cup. A different height step h_j can also be selected for each j, so that additional parameters such as overlap regions are considered in the design. The presented version of the algorithm was a simple one, where the number of delay classes κ was given a priori. Other versions of the algorithm may not assume a given number of delay classes and derive it as:

$$\kappa = \min\left\{\omega : cos^{-1}\left(1 - \frac{\sum_{i=0}^{\omega} h_i}{R_E}\right) \leq \theta_{min}\right\} \tag{10}$$

This denotes that the satellite footprint is sequentially covered with delay classes until angle θ_{min} is reached.

VIII. Appendix B : UT position determination using delay and Doppler frequency

Let $\vec{P}(t)$ and $\vec{S}(t)$ be the UT and satellite position vectors at time t. Denote by $\vec{D}(t) = \vec{S}(t) - \vec{P}(t)$ and t_d the distance and propagation delay from the UT to the satellite, f_d the Doppler frequency offset because of movement of the satellite and f the frequency. Then, the delay t_d and Doppler offset f_d are [14],

$$t_d = \frac{|\vec{D}(t)|}{c} = \frac{|\vec{S}(t) - \vec{P}(t)|}{c} \ , \ f_d = -\frac{\vec{D}'(t)}{c} f \tag{11}$$

where $\vec{D}'(t)$ is the derivative of $\vec{D}(t)$. UT position is typically given in terms of UT longitude and latitude. An alternative form of UT position can be given by defining the following angles (Fig. 13):

- The *distance angle* a of UT from the sub-satellite point Q, which shows UT distance from satellite nadir.
- The *azimuth angle* b of a UT at the sub-satellite point relative to the direction of satellite motion.
- The *instant position angle* w, which gives the position of a satellite in its orbit plane as time t as $w(t) = 2\pi t/T$, where T is the period of revolution of the satellite.

Let $\vec{Q}$ be the vector corresponding to the sub-satellite point Q. Delay is computed with the law of cosine,

$$t_d = \frac{\sqrt{R_E^2 + (R_E + H)^2 - 2R_E(R_E + H)\cos a}}{c}. \tag{12}$$

To calculate the Doppler frequency offset, the representation of $\vec{P}(t)$ through a, b and w (Figure 13) is transformed to Cartesian coordinates. For simplicity, we do not show the time dependence of $\vec{P}$ and $\vec{S}$. The transformation is done in three stages:

1. Assume that the sub-satellite point Q is initially at the intersection of equator and Greenwich meridian and the satellite orbit plane is the xy-plane, so that the ground track (projection of satellite movement on the earth) coincides with the equator. Then, the coordinates of $\vec{P}$ ($\vec{P}_1$, in this first stage) are

$$x_{p,1} = R_E \cos a \ , \ y_{p,1} = R_E \sin a \cos b \ , \ z_{p,1} = R_E \sin a \sin b \tag{13}$$

2. Multiply $\vec{P}_1$ with matrix A_1,

$$A_1 = \begin{bmatrix} \cos w & -\sin w & 0 \\ \sin w & \cos w & 0 \\ 0 & 0 & 1 \end{bmatrix}, \tag{14}$$

to define a rotation of $\vec{P}_1$ (and $\vec{Q}$) with respect to z-axis, so that Q has an angle w with respect to the x axis. After this rotation, we get vector $\vec{P}_2 = A_1 \cdot \vec{P}_1$.

3. Assume that satellite orbit has inclination angle i with respect to x-axis. Multiply $\vec{P}_2$ with matrix A_2,

$$A_2 = \begin{bmatrix} 1 & 0 & 0 \\ 0 & \cos i & -\sin i \\ 0 & \sin i & \cos i \end{bmatrix}, \tag{15}$$

to define this rotation. Then, $\vec{P}_3 = A_2 \cdot \vec{P}_2$. After combining these equations, we obtain coordinates x_p, y_p and z_p and vector $\vec{P} = (x_p, y_p, z_p)$, where the latter depends on time, through $\omega(t)$. UT motion can then be described with vector $\vec{P}'(t) = d\vec{P}(t)/dt$.

Point $\vec{Q}$ can be considered to be a special point $\vec{P}$ with $a = 0$. Recall that Q is the projection of the satellite (vector $\vec{S}$) on the earth. Vector $\vec{S}$ can be expressed in terms of a, b, and w as:

$$\vec{S} = (R_E + H) \begin{bmatrix} \cos w \\ \sin w cosi \\ \sin w \sin i \end{bmatrix} \tag{16}$$

and we find the motion $\vec{S}'$ of the satellite, given the time dependence of $w(t)$. After some algebraic manipulations we can show that $(\vec{S} - \vec{P})(\vec{S}' - \vec{P}') = 2\pi(R_E + H) \sin a\gamma$, Therefore, the Doppler Frequency shift can be computed as $f_d = \gamma(b, \omega) \cdot g(\alpha)$, where $g(\alpha)$ and $\gamma(b, \omega)$ are given by

$$g(\alpha) = -\frac{2\pi R_E (R_E + H) f \sin a}{c\sqrt{R^2 + (R_E + H)^2 - 2R_E(R_E + H)\cos a}}, \quad \gamma(b, \omega) = \left(\frac{\cos b \cos i - \cos w sinb \sin i}{T} - \frac{\cos b}{T} \right) \tag{17}$$

Given the satellite position $\vec{S}$, the measured delay t_d and Doppler frequency shift f_d, the UT position $\vec{P}(t)$ can be determined as follows:

- Step 1 : Compute angle a from (12).
- Step 2 : Solve equation $f_d = \gamma(b, \omega) \cdot g(\alpha)$ for b.
- Step 3 : Calculate w from equation (16).
- Step 4 : Transform (if desirable) the (a, b, w) representation of $\vec{P}$ to an alternative representation (e.g. latitude and longitude) for verification.

References

[1] F. Ananasso and F. Delli Priscoli, "The role of satellites in personal communication services", *IEEE Journal on Selected areas in Communications,* vol.13, no.2, pp.180-196, 1995.

[2] M. Werner, A. Jahn, E. Lutz and A. Böttcher, "Analysis of system parameters for LEO/ICO Satellite communication networks", *IEEE Journal on Selected areas in Communications,* vol.13, no.2, pp.371-381, 1995.

[3] N. Bains, "The ICO system for personal communications by satellite", 6^{th} *International Mobile Satellite Conference,* 1999.

[4] P. Carter and M.A. Beach, "Evaluation of Handover mechanisms in shadowed Low Earth Orbit Land Mobile satellite systems", *International Journal of Satellite Communications,* vol.13, pp.177-190, 1995.

[5] J. Restrepo and G. Maral, "Coverage concepts for satellite constellations providing communications services to fixed and mobile users", *Space Communications,* vol.13, no.2, pp.145-57, 1995.

[6] K. N. Sivarajan, R. J. McEliece and J. W. Ketchum, "Channel assignment in cellular radio", *IEEE 39th Vehicular Technology Conference,* 1989.

[7] R. Mathar and J. Mattfeldt, "Channel assignment in Cellular radio networks", *IEEE Transactions on Vehicular Technology,* vol. 42, no. 4, pp. 647-655, 1993.

[8] S. Tekinay and B. Jabbari, "Handover and Channel assignment in mobile cellular networks", *IEEE Communications Magazine,* vol.29, no.11, pp.42-46, 1991.

[9] E. Del Re, R. Fantacci and G. Giambene : *Efficient Dynamic Channel Allocation techniques with Handover Queuing for mobile satellite networks*, IEEE Journal on Selected areas in Communications, vol.13, no.2, pp.397-405, 1995.

[10] E. Del Re and P. Iannucci, "The GSM procedures in an integrated cellular/satellite system", *IEEE Journal on Selected areas on Communications,* Vol.13, No.2, pp.421-431, Feb. 1995.

[11] T. E. Wisloff, "Dual Satellite path diversity and practical channel management for non-geostationary satellite systems", *5th IEEE International Conference on Universal Personal Communications,*, 1996.

[12] W. Zhao and S. P. Arnold, "Timeslot assignment for GEO Mobile (GEM^{TM}) Satellite system", *Sixth International Mobile Satellite Conference,* 1999.

[13] I. Koutsopoulos and L. Tassiulas, "A synchronization-based scheme for simultaneous full- and half-duplex communication in GSM-based MEO Mobile Satellite networks," *GLOBECOM* 1999.

[14] D. Roddy, "Satellite Communications", Mc Graw-Hill, 1996.

[15] A. Böttcher and M. Werner, "Strategies for Handover control in Low Earth Orbit Satellite systems", *IEEE 44th Vehicular Technology Conference,* 1994.

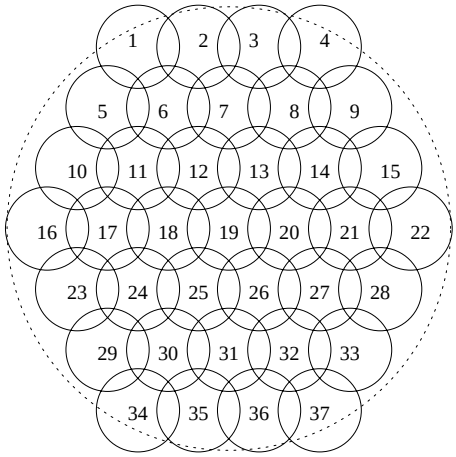

Fig. 1. Classification of beams of a satellite footprint in beam types.

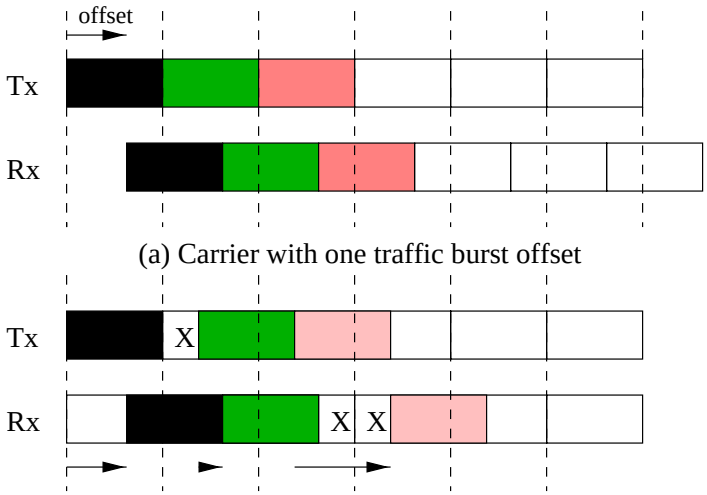

Fig. 2. Comparison of the cases of single and multiple burst offset values.

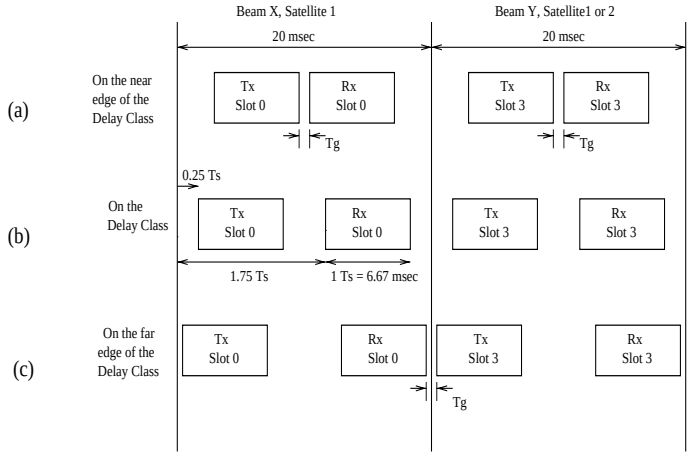

Fig. 3. Relative positions of transmission and reception traffic bursts in a reference window for three users in the same delay class.

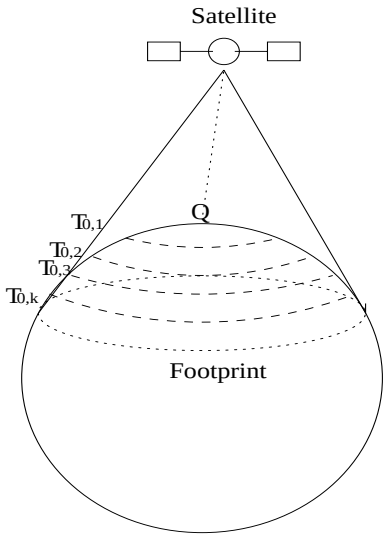

Fig. 4. Different delay classes within a satellite footprint.

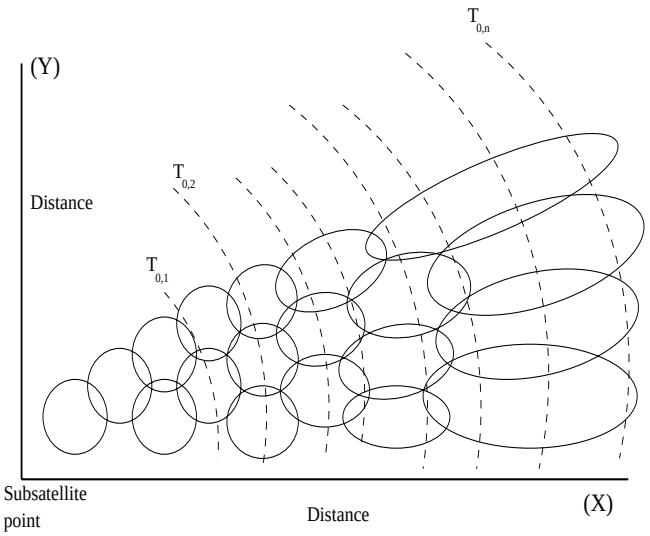

Fig. 5. Relative position of delay classes and beams in the satellite footprint.

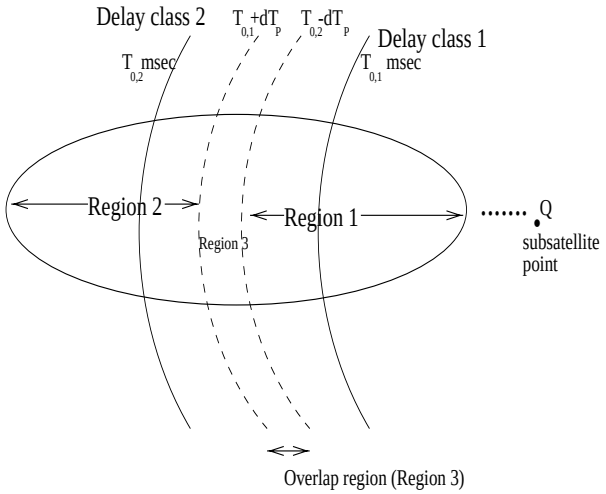

Fig. 6. A beam with two delay classes and the corresponding overlap region.

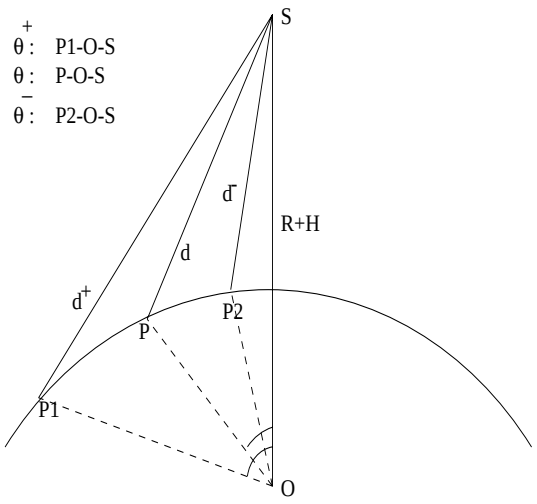

Fig. 7. Algorithm A: Computation of the amount of tolerance in UT position inaccuracy.

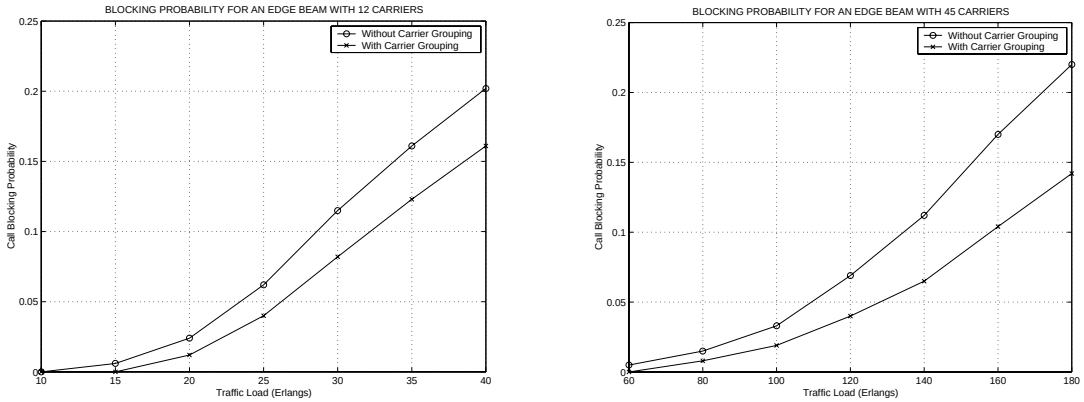

Fig. 8. Blocking rates with and without the carrier grouping method, for an edge beam with 12 and 45 carriers.

TABLE I

PERCENTAGE OF TIMES WHEN THE UT LIES WITHIN A CERTAIN RANGE OF DISTANCE FROM ITS ACTUAL POSITION FOR DIFFERENT UT POSITION DETERMINATION METHODS

Method	$<$ 25km	$<$ 50km	$<$100km	$<$ 150km
M. I	82%	92%	96%	97%
M. II	82%	93%	96%	98%
M. III	90%	95%	97%	98%
M. IV	84%	95%	98%	99%
M. V	85%	94%	97%	99%
M. VI	64%	93%	99%	$>99\%$
M. VII	97%	93%	$>99\%$	$>99\%$

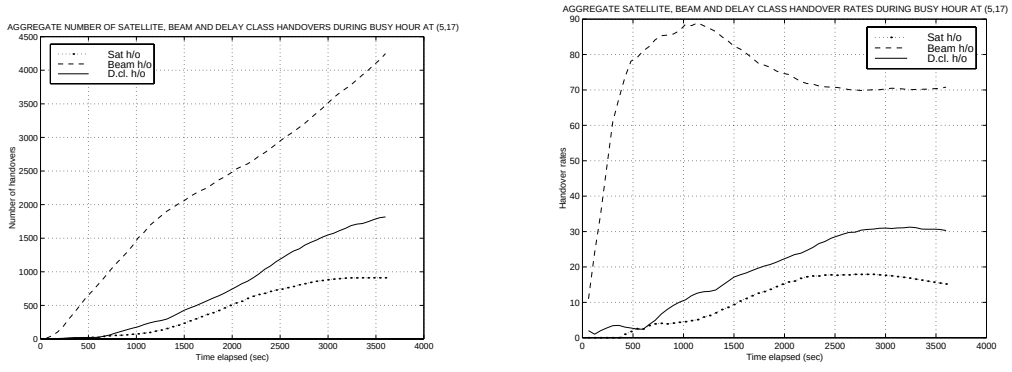

Fig. 9. Satellite, beam and delay class handover: number of handovers and handover rates at a square region within 15^o longitude and latitude distance from the GW, where $\lambda = 4.87$ calls/sec.

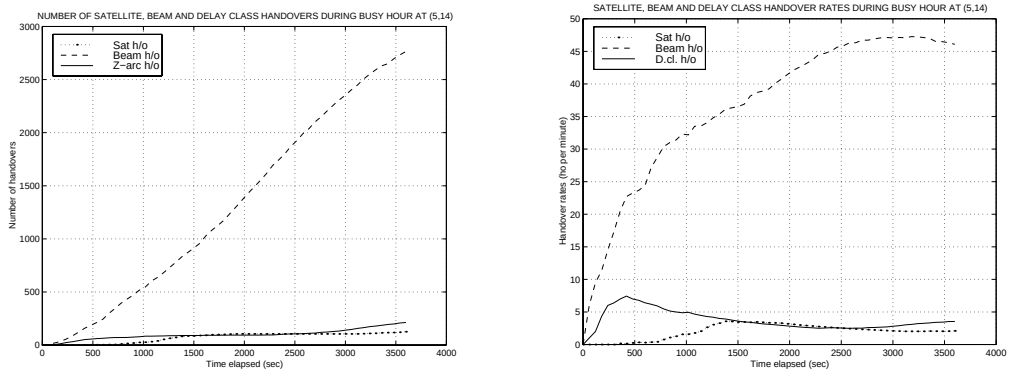

Fig. 10. Satellite, beam and delay class handover: number of handovers and handover rates at a square region $(15^o, 30^o)$ longitude, $(15^o, 30^o)$ latitude within 45^o longitude and latitude distance from the GW, where $\lambda = 1.69$ calls/sec.

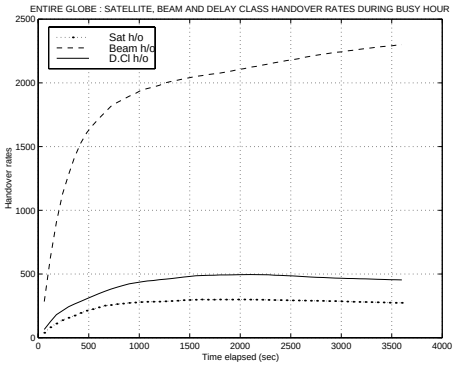

Fig. 11. Aggregate satellite, beam and delay class handover rates for all calls served by a particular GW.

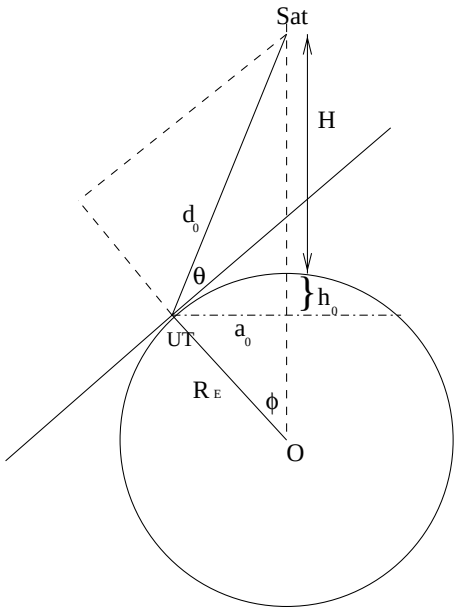

Fig. 12. Algorithm C: delay class determination. Illustration of first step.

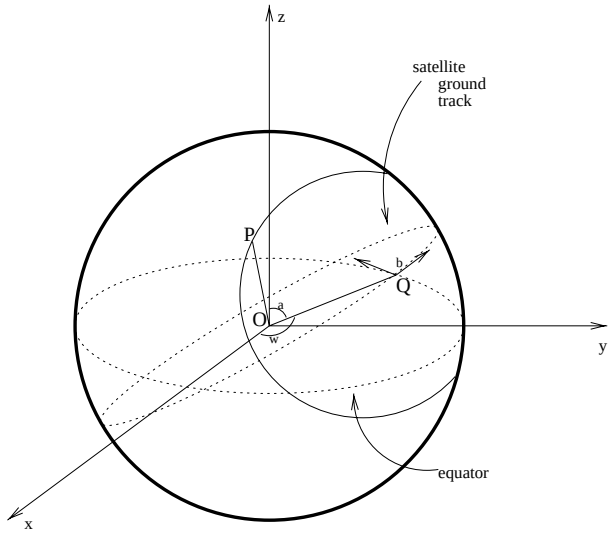

Fig. 13. Required angles for UT position computation.